Original Research Article

Glibenclamide-Loaded Polyvinylpyrrolidone (PVP) Nanoparticles and Glibenclamide-Loaded Soluplus® Nanomicelles Intended for Parenteral Administration: Effect of Solvents mixtures on the Electrosprayed Nanoparticles and *In Vitro* Characterization

Formatted: Font: Italic

Abstract:

Background and Objective: Glibenclamide (GB~~) is~~) is showing promising results in central nervous system (CNS) injuries treatment where intravenous administration of GB could overcome the oral limitations and assure maximum bioavailability. Dry powder of GB nanoparticles reconstituted for parenteral administration was prepared through electrospraying.

Methods: The drug was incorporated with two polymers, polyvinylpyrrolidone (PVP) and Soluplus® (SP), at ratios 1:4 and 1:2 (GB/polymer). Different solvents mixtures were used to formulate the particles. Physicochemical characteristics were investigated.

Formatted: Superscript

Results: The size of the GB-PVP nanoparticle ranged between (409-775) nm with a spherical, disk, fractured and, agglomerated morphology, while those of the GB-SP nanomicelles were of (447-785) nm with mostly irregular morphology, in consequence to the used solvents mixtures. The high encapsulation efficiency ≥ 98% reflects the well dispersed drug molecules within the polymer matrix, further confirmed by X-ray diffraction and infrared spectroscopy. GB-SP

colloidal dispersions showed neutral zeta potentials with a cloud point of 36 ˚C, indicating prolonged circulation time and stability after parenteral administration. GB/SP nanomicelles at ratio 1:4 showed a sustained drug release reaching ≥ 94% in 36 hours.

Conclusion: The GB-SP nanomicelles with extended drug release and regarding physicochemical properties represent a remarkable drug delivery system for parenteral administration.

Keywords: glibenclamide; Soluplus®; polymeric nanomicelles; electrospraying; parenteral administration; nanoparticles; PVP

1. **Introduction:**

Nanoparticles are promoting drug delivery systems via enteral, parenteral, nasal, or transdermal routes of administrations. The particle size [1] and the shape [2] control the drug release and bioavailability. Practically speaking are poorly water-soluble drugs, through using different methods of manufacturing that utilize varied ways of preparation, it could be implemented by particle engineering. The nanoparticles produced by atomization methods, such as spray drying and electrospraying, are being governed by the used solvents.

Electrospraying is a novel method, provides a great candidate to generate nanoparticles drugs with one step, less time, high yield, high encapsulation, and is suitable to all (API) [3]. Leaning on the solvent properties of boiling point, electrical conductivity, and surface tension, exerting electrical potential to the solution of these solvents drive versatile particle shapes [4]–[7]. According to the electrostatic principle, a liquid solution is fed through a capillary nozzle where it is being subjected to a high voltage, charging the liquid surface of the droplet with high

electrical stress obliging the droplet to elongate, forming a liquid jet. When the Rayleigh limit ΦRay (the electrical stress on the droplet surface overcomes the surface tension of the droplet), is reached coulomb fission took place to generate particles in micro- to nano-scale [8]. The electrospraying process essentially depends on the solvent or solvent blends used, also the amount or the ratio of different solvents blends.

Glibenclamide (GB) is a poorly water-soluble drug type II according to Biopharmaceutics classification system (BCS) [9]. It is a second generation sulfonylurea that binds to the sulfonylurea receptor (SUR) subunit of adenosine triphosphate (ATP) sensitive potassium channels (KIR6.2/KCNJ11) [10]. GB is mainly used as an oral drug to treat second type, diabetes patients. Nowadays, GB is showing promising results in central nervous system (CNS) injuries treatment. Where SUR1-TRPM4 channel was reported to be formed in CNS injured cells being liable to the inhibition of sulfonylurea [10], [11]. The formation of this channel was described in different cell types of CNS injury, including subarachnoid hemorrhage, stroke, intracranial hemorrhage (ICH), traumatic brain injury (TBI), and encephalitis [10]–[12]. The action of GB is to inhibit the SUR1-TRPM4 channel activation that leads to oncotic edema and then cell blebbing and oncotic cell death. A major drawback of oral GB administration is the absorption time of nearly nine hours, which demands higher dosing and incorporates delayed effect, nonetheless the functional obstacle of an unconscious patient as in stroke patient to sallow a pill [13]. Parenteral administration of GB as IV administration could overcome the oral limitations and assure maximum bioavailability.

Administer two polymers; one is soluble in water Polyvinylpyrrolidone (PVP) and a novel amphiphilic polymer Soluplus® (SP). Soluplus® is a graft copolymer of polyvinyl caprolactam-polyvinyl acetat-e-polyethylene glycol (PEG 6000/ vinyl caprolactam / vinyl

acetate) in the ratio (13/ 57/ 30) [14]. Soluplus® is a polymeric micelles consisting of both hydrophilic and lipophilic polymers in core/shell structures [15]. The SP tends to form micelles in nanoscale at concentrations higher than the critical micelles concentration (CMC). The poorly water-soluble drug is encapsulated in the lipophilic core, increasing its solubility and stabilizing the drug in the supersaturated state, inducing a more sustained release [16]. Polymeric micelles showed longer blood circulation periods, slowly releasing the drug. They inhibit P-glycoprotein at drug-resistant tumors, gastrointestinal tract, and blood-brain barrier, which may give a route to prevail over drug resistance in cancer and increase drug absorption from the gut and drug absorption into the brain [17]. These properties referred to the hydrophilic part of the polymeric micelles, especially the polyethylene glycol (PEG) moiety as in Soluplus® [15].

The PVP, SP~~, and~~, and GB are of different solubility in many organic solvents, and each solvent is unique in its properties participating in developing versatile particles in size and morphology. Binding two solvents, miscible with each other, to form a mixture would propagate their properties. So, by choosing three blends of solvents and changing the (drug/ polymer) ratio while fixing the concentration of the solute, we anticipate nanoparticles of different physicochemical characteristics and so of drug release.

Electrosprayed SP has never been studied in comprehensively to explore the particle size, morphology, or the type of the used solvents [18]–[20]. To the best of our knowledge, there are no reports in which nanomicelles of glibenclamide were formulated with Soluplus® [21]–[23]. Also, this is the first time to study the effect of different solvents mixtures on the electrosprayed SP nanomicelles and PVP nanoparticles. This study aims to produce GB-PVP nanoparticles and GB-SP nanomicelles as dry powder injections for reconstitution formulations.

2. Materials and Methods:

2.1 Materials:

Glibenclamide powder was purchased from Shanghai Ruizheng Chemical Technology Co., Ltd (Shanghai, China), Polyvinylpyrrolidone PVP K30 (MW= 30000 g/mol) was purchased from Central Drug House (P) Ltd. (New Delhi, India). Soluplus (MW= 118000 g/mol) was purchased from BASF SE (Ludwigshafen, Germany). Ethanol absolute anhydrous from Carlo Erba Reagents S.A.S (Val de Reuil Cedex, France), Methanol A.R. from Chem-Lab NV (Zedelgem, Belgium), Acetone from Alpha Chemika (India) and Potassium dihydrogen orthophosphate Hi-LR (MW= 136.09 g/mol) was procured from Himedia Laboratories Pvt. Ltd. (Mumbai, India). Methanol, Methylene Chloride extra pure and Sodium hydroxide purified pellets LR (MW= 40,000) were acquired from Thomas Baker Chemicals Pvt. Ltd. (Mumbai, India). All chemicals and reagents used were of analytical grade and were used as received without any further purification.

Comment [U1]: 40.00 g/mol?

2.2 Preparation of solvents mixture solutions:

A solution of 2% (w/v) concentration was prepared for electrospraying, where GB in the ratio of 1:4 and 1:2 (w/w) (drug/ polymer) was added to the solution of two solvents blend. The drug was added first under a magnetic stirrer for one hour to fully solubilize it, then the polymer was added and left on the stirrer for another hour. The PVP and SP were selected as the carriers. PVP is insoluble in acetone (Act) but does solubilize in many other organic solvents such as methanol (MeOH) and ethanol (Eth). Blends of (Act/Eth) and (Act/MeOH) in different ratios were prepared with (GB/PVP). Methylene chloride or dichloromethane (DCM) is a good solvent for both GB and PVP. Solutions of (GB/PVP) in (DCM/MeOH) and (DCM/Eth) with varied ratios

were made. Solutions of SP in Act blends and DCM blends were prepared in the same procedure as with PVP. The physical properties of the used solvents are shown in Table. 1.

Table. 1. The physical properties of the solvents used in this study [3], [24]–[26].

Comment [U2]: Which temperature for dielectric, viscosity and conductivity?

Formatted: Tab stops: Not at 3.25" + 6.5"

Solvent	Boiling point (˚C)	Dielectric constant	Viscosity (mPa.sec)	Electrical conductivity ($\mu S.cm^{-1}$)
Acetone	56	20.7	0.32	0.06
Ethanol	78	24.6	1.2	0.0013
Methanol	65	32.6	0.57	0.5
Dichloromethane	40	10.7	0.44	0.00028

2.3 Electrospraying process setup:

Nanoparticles of the selected solvents mixtures solutions were obtained through a horizontal single nozzle electrospraying setup. A disposable plastic syringe of 1 ml and stainless steel needle of 30 G gauge diameter was loaded with the solution. The flowrate was fixed at 0.1 ml/hr using a syringe pump (Model no.300, New Era Pump Systems, USA). The applied voltage ranged between (6.5- 8.5) kV (HV350REG Positive, Information Unlimited, USA) for all the experiments and it was adjusted to establish and maintain a cone jet. The distance from the apex of the jet to the grounded plate was fixed at 8 cm. The process was carried out within room ambient conditions. The jet was monitored by a digital microscopic camera (Splaks, China), to guarantee the stable and continuous cone jet throughout the electrospraying.

2.4 Characterization of The Electrosprayed particles:

2.4.1 Characterization of Particle Size and Morphology:

The particle size and morphology were characterized through a field emission scanning electron microscope (FESEM) (Mira3, Tescan, France). The samples were prepared by taking a thin layer of particles, sputtered with gold and mounted on metallic stubs with double-sided carbon tape, and were viewed at an accelerating voltage of 15 kV. The obtained images were used to determine the mean diameter of the nanoparticles. About 200 particles from different sites of each sample were used to determine the particle size and size distribution by utilizing ImageJ software.

2.4.2 X-RAY Powder Diffraction (XRPD):

The diffraction patterns of the pure GB, PVP powder, SP powder, physical mixtures of GB/PVP (PM PVP) and GB/SP (PM SP) in the ratio 1:4 and 1:2 (w/w), and the samples of GB-PVP and GB-SP nanoparticles of the defined solvents mixtures were analyzed using the PANalytical X'Pert PROMPD system (PW3040/60, Philips, the Netherlands) employing Cu Kα radiation (λ= 1.542 Å). The measurements were carried out in the reflection mode 2θ in the range (10˚- 80˚) scanned at 40 kV and 30 mA. The scanning rate was 4 ~~min~~ min^{-1}~~1~~.

Formatted: Superscript

2.4.3 Fourier Transform Infrared Spectroscopy (FTIR):

The type of interaction between the drug and the polymer was studied by using FTIR. Samples were pure GB, PVP powder, SP powder, a physical mixture of GB-PVP powder and GB-SP powder, and electrosprayed GB-PVP and GB-SP nanoparticles of different solvents mixtures. A

sample of 2 mg was mixed with 10 mg of potassium bromide, compressed into a disk, and placed in the device (8400S, Shimadzu, Japan). The scanning range is (4000- 400) cm^{-1}.

Chemometric analysis: All the FTIR spectra were treated with multivariate analyses (MVA), specifically hierarchical cluster analysis (HCA) and principal component analysis (PCA), performed with the utilize of the OriginPro 2019b software (OriginLab, Northampton, MA, USA).

2.4.4 Drug Loading and Encapsulation Efficiency:

The drug loading (DL%) and encapsulation efficiency (EE%) was determined by taking 5 mg of each of the GB-PVP and GB-SP electrosprayed nanoparticles formulated with the selected solvents mixtures, then they were fully solubilized in 10 ml methanol under magnetic stirring for 5 minutes. The drug content of the nanoparticles was quantified by UV- visible spectrophotometer (Cary 100, Varian, USA). The DL% and EE% were calculated by Eqs. (1) and (2), respectively:

DL% = (Weight of GB in nanoparticles / (Weight of GB fed + Weight of the polymer)) × 100 (1)

EE% = (Weight of GB in nanoparticles / Weight of GB fed) × 100 (2)

Three replicates were used to determine the result which was indicated by the mean value ± SD.

2.4.5 Reconstitution of Dry Powder Injection:

The GB-PVP nanoparticles and GB-SP nanomicelles powder was reconstituted with distilled water to obtain a solution of 5 (mg/ml) and 3 (mg/ml) for GB loading of 25% and 50%, respectively. The samples were gently shaken by hand for (1-2) minutes until a clear solution

was established. The samples were sonicated for a few minutes to confirm the complete dispersion of the powder.

2.4.6 Zeta-potential:

The zeta potential of the GB-PVP nanoparticles and GB-SP nanomicelles were conducted by nanopartica series instruments (HORIBA SZ-100, Japan). A sample of 5 ml of each reconstituted powder formulation was tested. Three measurements were made, and the average value ± SD was calculated.

2.4.7 Cloud Point of Micelles Formulation:

The cloud point value of GB-SP nanomicelles was determined by submerging glass tubes containing 5 ml of the reconstitution powder in a water bath at room temperature. Subsequently, the temperature was increased till the point of rapid change from clear to turbid. Then, the samples were cooled down, and the measurements were repeated to obtain a triplicate [16], [27].

2.4.8 Drug Release Study:

The *in vitro* drug release was conducted through the dialysis bag method. Five ml of GB-PVP and GB-~~SP reconstituted~~SP reconstituted powder were added to a dialysis membrane (regenerated cellulose, Special Products Laboratory, China, MWCO 8-14 KD). The dialysis membrane was then immersed in 100 ml of the release media at 37 ˚C under magnetic stirring at 100 rpm. The 0.05 M PH 7.4 sodium phosphate buffer (PBS) was selected as the release media. At a predetermined time intervals, 2 ml of the release medium was withdrawn for UV analyses

Formatted: Font: Italic

and replaced with the same volume of fresh media. A reading was made at 300 nm. The cumulative release was calculated according to Eq. (3):

$$\text{Cumulative release\%} = (M_t / M_\infty) \times 100 \quad (3)$$

Where M_t is the total amount of GB that had been released in the medium, including the amount being sampled at every time point, and M_∞ is the initial GB amount in the dialysis membrane. At least three replicates were used to determine the release indicated by mean value ± SD.

The data obtained from the dissolution tests were fitted into various mathematical models such as zero-order, first-order, Higuchi, Korsmeyer–Peppas, and Baker–Lonsdale models to demonstrate the drug release mechanism from the different formulations. The best fit was granted for the highest correlation coefficient (R^2) value model.

3. Results and Discussion:

Particles produced with different solvents mixtures reflect the properties of the used solvents, as the solution mainly consists of solvents. Electrospraying is being governed by two types of parameters~~, process~~, process parameters, and formulation parameters. The type of solvent is a key factor in formulating particles in the desired specifications such as size and shape. Each solvent has unique physical properties of boiling point, surface tension, electrical conductivity, and viscosity which dominate the formulation parameters with the solute concentration and by interacting with the process parameters (the voltage, the flowrate, the distance from the nozzle to the collector, and the nozzle gauge) a stable Taylor cone jet is established. The used polymer, on the other hand, being the matrix where the process develops, has a large share in conducting particle size and morphology depending on its concentration and the molecular weight through

the chains entanglement within the confined solvents.

3.1 Mapping of Solvents Mixtures:

The selection of solvents was based on the solubility of GB and the polymers. The Act and DCM solubilize GB to about 40 mg ml^{-1} and 80 mg ml^{-1}, respectively. The solubility test was made by adding a small amount of GB to 10 ml of either the solvents and mixed by a magnetic stirrer. The addition of GB continued until a turbid solution appeared. GB is of poor solubility in Eth (3 mg ml^{-1}) and MeOH (4 mg ml^{-1}). Blending of Act with either Eth or MeOH in the ratio (8/2) ml elevated the solubility power of GB to 100 mg ml^{-1}. The same trend was obvious with DCM.

Comment [U3]: EtOH? Ethanol?

PVP is insoluble in Act. Different blends of Act with a soluble solvent (either Eth or MeOH) were prepared to assess the effect on the characteristics of the electrosprayed nanoparticles. Both Eth and MeOH do solubilize PVP up to 100 mg ml^{-1}. The (Act/ Eth) or (Act/MeOH) mixture, in the ratio of 8/2 ml, was chosen to assure the full solubility of the solute. The DCM is a good solvent for both GB and PVP, but its low boiling point of about 40 ˚C and low dielectric constant of 10.7 (Table. 1) causes difficulty in creating a stable cone jet [28]. It is more suitable to mix it with another miscible solvent of appropriate physical properties to initiate a continuous steady electrospraying process. The mixture of (DCM/ MeOH) in the ratio 8/2 ml was challenging to start and maintain a cone jet, where a very stressed jet showed up. A (DCM/Eth) mixture, in the ratio of 4/6 ml, was chosen to work with to state the effect of the boiling point on structuring the particles.

The same solvent blends and their ratios were used to make (GB/SP) electrospraying solutions to facilitate the comparison of the obtained nanomicelles with the GB-PVP nanoparticles. The electrical conductivity and surface tension values of GB-PVP and GB-SP

solutions in different solvents mixtures are shown in (Table. 2). There was no such a variation between the two polymers solutions, while there was an inherited difference between the solvents mixtures for the same polymer solution regarding the solvents being used. The DCM/Eth and DCM/MeOH solvents showed the lowest electrical conductivity, which was reflected in the electrospraying of their solutions.

3.2 Particle Size and Morphology:

The nanoparticle size of PVP and SP systems is shown in Table. 3. For PVP, the (Act/MeOH) mixture, flat disk-shaped particles were obtained for GB loading of 25 % (w/w) and fractured nanoparticles for 50 % (w/w) (Fig. 1 a & b). The low boiling points of Act and MeOH of 56 ˚C and 64 ˚C, respectively (Table. 1), gave less time to full chains entanglement, and so the particles collapsed into flat particles, and the fractured ones were obtained as a result of the low supporting matrix of PVP. The insolubility of PVP in Act that represents the large portion of solvents mixture could make the polymer precipitated compactly, while GB is moving in the droplet around and within the compacted polymer molecules [29]. As the Act portion is about to

Table. 2. Electrical conductivity and surface tension of GB-PVP and GB-SP solutions prepared for electrospraying.

PVP				
Solvent mixture (v/v)	Drug loading (%)	Polymer concentration (%)	Electrical conductivity ($\mu S\ cm^{-1}$)	Surface Tension ($mN\ m^{-1}$)
Act/Eth (8/2)	25	1.6	3.9	22.9
Act/Eth (8/2)	50	1.3	3.7	23.2
Act/MeOH (8/2)	25	1.6	5.3	22.4
Act/MeOH (8/2)	50	1.3	4.5	22.1
DCM/MeOH(8/2)	25	1.6	2.8	21.9
DCM/MeOH(8/2)	50	1.3	2.5	22.4

DCM/Eth (4/6)	25	1.6	1.7	23.3
DCM/Eth (4/6)	50	1.3	1.5	22.8
SP				
Act/Eth (8/2)	25	1.6	4.1	21.6
Act/Eth (8/2)	50	1.3	3.8	21.4
Act/MeOH (8/2)	25	1.6	5.7	22.3
Act/MeOH (8/2)	50	1.3	5.2	22.4
DCM/MeOH(8/2)	25	1.6	3.1	23.2
DCM/MeOH(8/2)	50	1.3	2.7	22.7
DCM/Eth (4/6)	25	1.6	1.9	22.5
DCM/Eth (4/6)	50	1.3	1.6	22.2

end, MeOH of good solubility of PVP is dominated now, and the polymer chains are more extended in the solvent. The PVP molecules, trying to diffuse toward the core of the droplet as the solvent evaporates, but the limited time due to the somewhat low boiling point of 64 ˚C makes the precipitated polymer at the shell of the droplet larger than the diffused molecules to the core eventually, the particle collapsed in a disk shape nanoparticle.

The mixture of Act/Eth delivered spherical particles (Fig. 1c & d) with the smallest size and less dispersity (Table. 3). Regarding PVP insolubility in Act and very well solubility in Eth, PVP chains are more extended into Eth, as it is the last solvent to be evaporated at 78 ˚C (Table. 1), giving sufficient time to full chains entanglements before reaching Φ_{Ray}. The viscosity of Eth is higher compared to MeOH with 1.2 mPa.sec and 0.56 mPa.sec, respectively (Table. 1). The higher viscosity of Eth with its good solubility of PVP supports the spherical integrity of the droplets. When contemplating the mixture of (DCM/MeOH) of 8/2 ml agglomerated particles, were recognized for GB loading of 25% (w/w) (Fig. 1 e). The hygroscopicity nature of PVP and the low boiling point of DCM shaped the nanoparticles. While for the GB loading of 50% (w/w), smaller nanoparticles with larger size distribution were produced (Fig. 1 f). The DCM is a good solvent of PVP and so the polymer chains extended in the solvent interacting as polymer/solvent

Comment [U4]: for

chains instead of the polymer/polymer chains interacting in the bad solvent, so spherical particles are expected to be obtained.

Remarkably, (DCM/Eth) in the ratio of 4/6 ml exhibited the largest particle size of 775 nm (Table. 3). The droplet size is dependent on the electrical conductivity according to the scaling law as shown in Eq. (4) [30]:

$$d_o = [\sigma \varepsilon_o^2 / \rho K^2]^{1/3} \quad (4)$$

Where d_o is the droplet diameter, σ is the surface tension, ε_o is the vacuum permittivity, ρ is the density, and K is the electrical conductivity. The low conductivity of both Eth and DCM is responsible for enlarging particle size even with a superior portion of Eth of the higher boiling point.

Particles produced with SP differ in size and morphology. The mixtures of (Act/MeOH) and (Act/Eth) in the ratio 8/2 ml delivered cup shape like nanoparticles for the GB loading of 25% (w/w) and deformed accompanied with clustered nanoparticles for 50 % (w/w) (Fig. 2 a-d). The (DCM/Eth) mixture in the ratio of 4/6 ml submitted the largest size with more even morphology of spherical to semispherical particles (Fig. 2 e). The high Eth share in the solvent blend with its high boiling point ensures the right time to the polymer chains entanglement and the polymer diffusion toward the center of the droplet opposite to the solvent evaporation, which is consistent with the Peclet number (Pe). Eq. (5) defines *Pe* as [31]:

$$\mathrm{Pe} = (\partial r_d/\partial t)\,(r_d)/\,D_{AB} \quad (5)$$

Where $\partial r_d/\partial t$ is the shrinkage rate of droplet surface, r_d is the droplet radius and D_{AB} is the diffusivity of the solute inside the droplet. The (Act/Eth) and (Act/MeOH) mixtures gave smaller droplet sizes due to their higher conductivity (Table 2 and Table 3), translated into less

Formatted: Font: Italic
Formatted: Font: Italic
Formatted: Font: Italic
Formatted: Font: Italic
Formatted: Font: Italic
Formatted: Font: Italic

evaporation time with an emphasis on the high volatility (low boiling point) solvent, which reduces this time more [31]. As a result cup shape nanoparticles were present.

The SP is of higher molecular weight than PVP with longer chains, and so the extended chains need more time to entangle while diffusing to the center of the droplet, so the insufficient evaporation time limits the completion of the chains entanglements before getting the Φ_{Ray} and collapsed particles (non-spherical) obtained.

3.3 Solid State of ~~The~~the Particles:

3.3.1 XRPD:

The composition of the GB-PVP nanoparticles and GB-SP nanomicelles were analyzed through XRPD to evaluate the drug state in the formulated solid dispersions. As depicted in (Fig. 3 a), the XRPD diffractogram of pure GB reflects the crystalline nature of the drug with high-intensity sharp peaks protruding in most at the diffraction angles (2θ˚) of 10.8˚, 11.7˚, 11.8˚, 19˚, 19.5˚, 21˚, and 23.2˚ [21]. These distinct peaks of GB are absent in the GB-PVP and GB-SP diffraction patterns (Fig. 3 a & b), which indicates the amorphous state of the drug and the complete dispersion within the polymer. The diffractograms of the physical mixtures showed the superposition of the reflections of both pure compounds, which imposes no interaction in the mixing process.

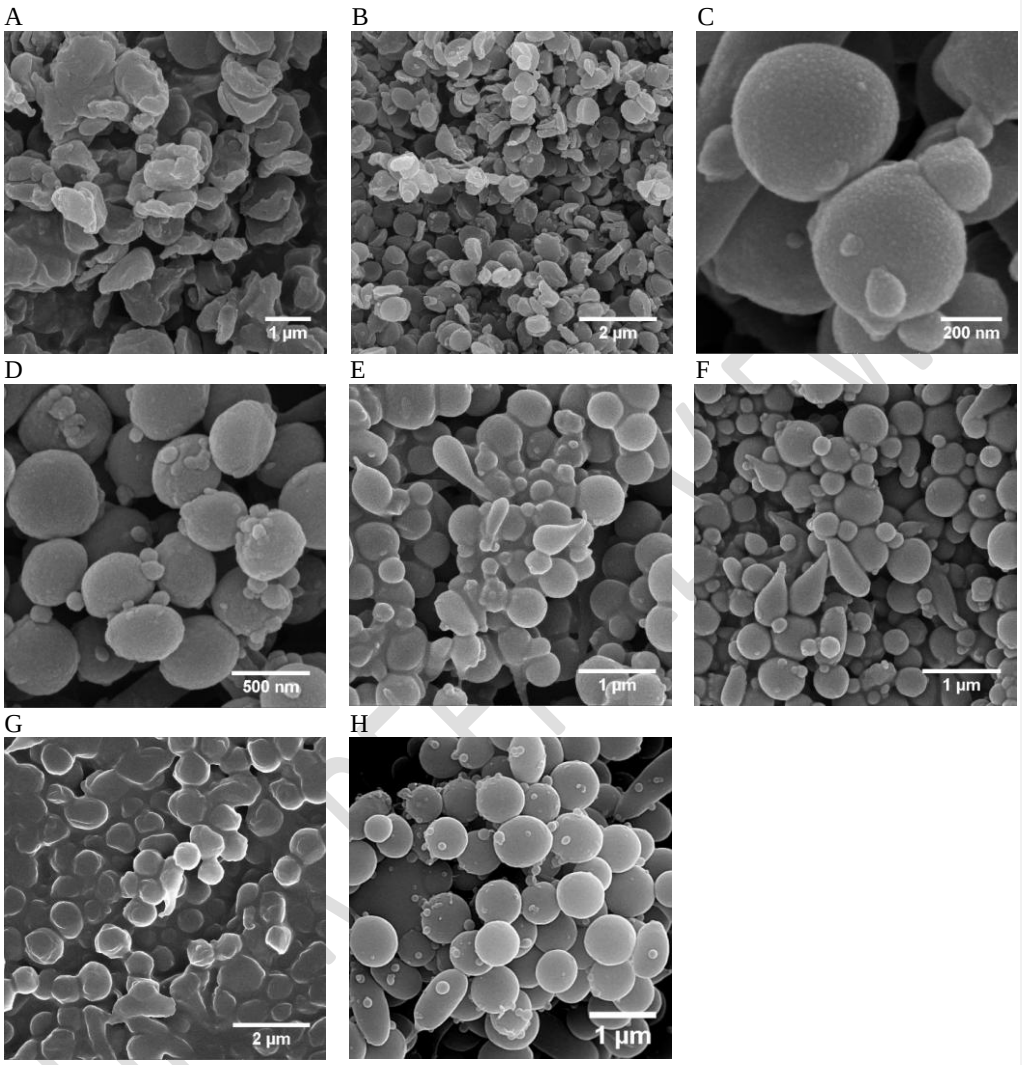

Fig. 1. FESEM images of GB-PVP nanoparticles prepared with Act/MeOH (A) S_{14} & (B) S_{15}, Act/Eth (C) S_{12} & (D) S_{18}, DCM/MeOH (E) S_{20} & S_{31}, and DCM/Eth (G) SEM_1 & (H) $SEM_{3/2}$.

Table. 3. Physical and chemical properties of GB-PVP nanoparticles and GB-SP nanomicelles.

All values are expressed as means ± SD (standard deviation).

PVP							
Sample No.	Solvents	GB content (%)	Particle size (nm)	Polydispersity Index (PID)	Entrapment efficiency EE (%)	Drug loading DL (%)	Zeta potential (mV)
S_{14}	Act/MeOH	25	467 ± 99	0.04	96 ± 2	19.2 ± 2	-33.23 ± 1.45
S_{15}	Act/MeOH	50	587 ± 282	0.23	97 ± 3	19.4 ± 3	-26.65 ± 2.83
S_{12}	Act/Eth	25	416 ± 62	0.02	100 ± 1	20 ± 1	-32.54 ± 2.11
S_{18}	Act/Eth	50	409 ± 48	0.01	99 ± 2	19.8 ± 1	-24.17 ± 1.98
S_{20}	DCM/MeOH	25	505 ±104	0.2	98 ± 3	19.6 ± 3	-32.13 ± 3.12
S_{31}	DCM/MeOH	50	429 ± 134	0.1	98 ± 4	19.6 ± 4	-26.82 ± 2.47
SEM_1	DCM/Eth	25	775 ± 122	0.02	99 ± 2	19.8 ± 2	-33.25 ± 1.61
$SEM_{3/2}$	DCM/Eth	50	647±117	0.03	99 ± 1	19.8 ± 1	-25.67 ± 2.27
SP							
SPE_3	Act/Eth	25	474 ± 146	0.09	100 ± 1	20 ± 1	-11.61 ± 2.41
$SPE_{3/2}$	Act/Eth	50	575 ± 322	0.31	101 ± 3	20.2 ± 3	-9.53 ± 1.75
SPM_2	Act/MeOH	25	543± 342	0.39	99 ± 2	19.8 ± 2	-11.48 ± 2.03
$SPM_{4/2}$	Act/MeOH	50	447 ± 157	0.12	100 ± 2	20 ± 2	-8.74 ± 2.53
EM_4	DCM/Eth	25	785 ± 186	0.05	99 ± 2	19.8 ± 2	-11.82 ± 1.66
$EM_{4/2}$	DCM/Eth	50	685±161	0.05	99 ± 1	19.8 ± 1	-9.12 ± 3.44

A B C

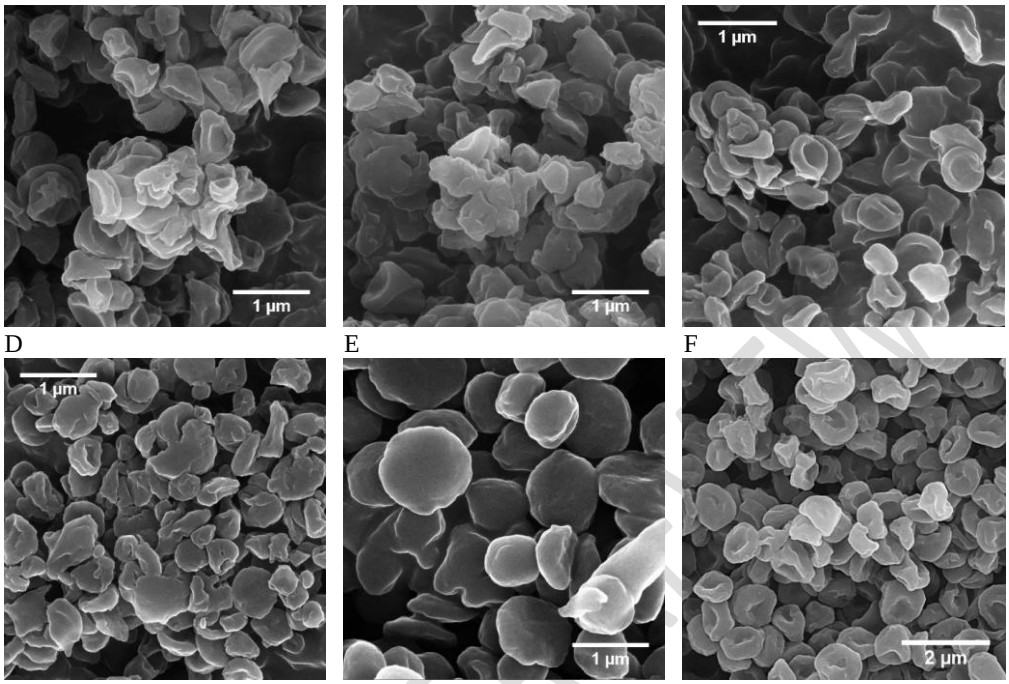

Fig. 2. FESEM images of GB-SP nanomicelles prepared with Act/Eth (A) SPE_3 & (B) $SPE_{3/2}$, Act/MeOH (C) SPM_2 & (D) $SPM_{4/2}$, and DCM/Eth (E) EM_4 & $EM_{4/2}$.

a

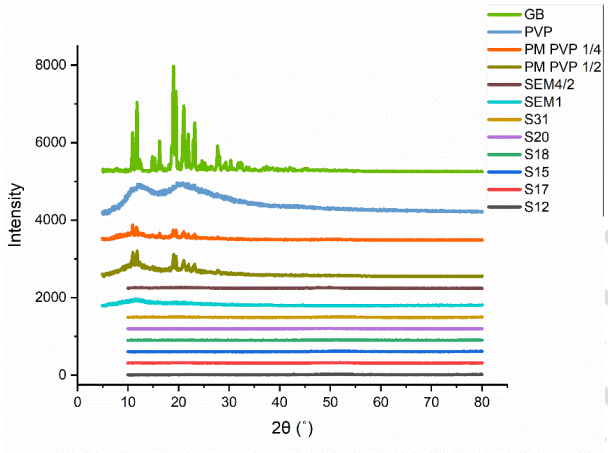

b

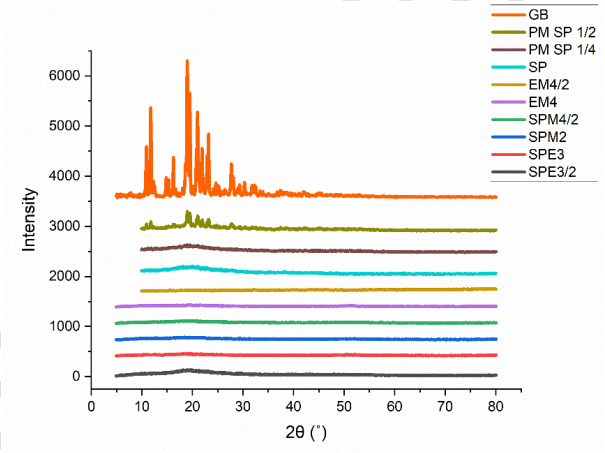

Fig. 3. The XRD diffractograms of (a): pure GB, PVP powder, physical mixture of GB/PVP (1:4) (w/w) PM PVP 1/4 & GB/PVP (1:2) (w/w) PM PVP 1/2, and GB-PVP nanoparticles and (b): pure GB, SP powder, physical mixture of GB/SP (1:4) (w/w) PM SP 1/4 & GB/SP (1:2) (w/w) PM SP 1/2, and GB-SP nanomicelles formulated with different solvents.

3.3.2 FTIR Analysis Supported by Chemometric Analysis:

FTIR tests were carried out to verify the molecular dispersion of the drug within the electrosprayed nanoparticles. The FTIR spectrums of GB-PVP nanoparticles and GB-SP nanomicelles are depicted in (Fig. 4 a & b), with pure GB, PVP powder, SP powder, and physical mixtures. Pure GB showed main absorption bands at 3369.75, 3315.74, and 1714.77 cm^{-1} that corresponded to NH, HN-C=O, and =C-O-C groups, respectively [32]. Observed peaks at 1159.26, 1184.33 cm^{-1} and distinct sharp peaks at 1305.85, 1344.43 cm^{-1} are correlated with the asymmetric and symmetric stretching vibration of SO_2 [22]. The urea N-H stretching vibrations are found at 1274.99, 1620.26, and 1529.26 cm^{-1}. The spectra of PVP exhibited O-H bending at 3448.84 cm^{-1}, C-H stretching band at 2955.04 cm^{-1}, and a characteristic carbonyl group at 1668.48 cm^{-1}. Spectra of Soluplus® showed inter-molecularly hydrogen-bonded–OH stretching in the range of 3275–3508 cm^{-1}, aromatic C-H stretching at 2928.08, ester carbonyl stretching at 1737.92 cm^{-1} and C=O stretching for tertiary amide at 1637.6 cm^{-1}, and C-O-C stretching at 1471.74 cm^{-1} [33], [34]. The FTIR spectra of physical mixtures were similar to those of pure GB and the individual polymer spectra, which strongly void the presence of chemical interaction.

The FTIR spectra of GB-PVP nanoparticles revealed the widening of the amide group at 3200-3500 cm^{-1} toward a high end wavenumber. The characteristic C=O stretching of PVP at 1668 cm^{-1} was persistent in all the nanoparticles as it was shifted to 1664-2 cm^{-1} with a lower intensity suggesting the hydrogen bonding. The distinguished GB peaks of 1159 (shifted to 1161-2), 1529 (shifted to 1535), 2852 (shifted to 2858-10) cm^{-1} were persevered in all GB-PVP nanoparticles. The low intense peaks indicate the hydrogen bonding between GB and PVP reflects the good drug dispersion.

IR spectra of the GB-SP nanomicelles (1:4) and (1:2) (w/w) showed the absence of the peaks at 3369, 3315, 1714, and 1620 cm^{-1}, where the N-H stretching peak of 3369 cm^{-1} interacts with the carbonyl group of SP at 1637 cm^{-1} through hydrogen bonding leading to the formation of amide group [35]. Soluplus characteristics peaks of 2928, 1737, and 1471 cm^{-1} were shifted with less intensity, suggesting the formation of hydrogen bonding with the drug. GB peaks at 1089.82 (shifted to 1091-6) and 1529 (shifted to 1531-2) cm^{-1}, which are not in the SP spectrum, were prominent in all the nanomicelles. The drug and the polymer interaction was an extra advantage for the nanomicelles. Not only inhibit the crystallization of the drug but improved the solid solubility of the drug into the hydrophilic matrix [33]. The results were consistent with the drug release results. The FTIR spectrum manifested the infallible encapsulation of the drug and that all the nanomicelles contained both GB and SP.

a

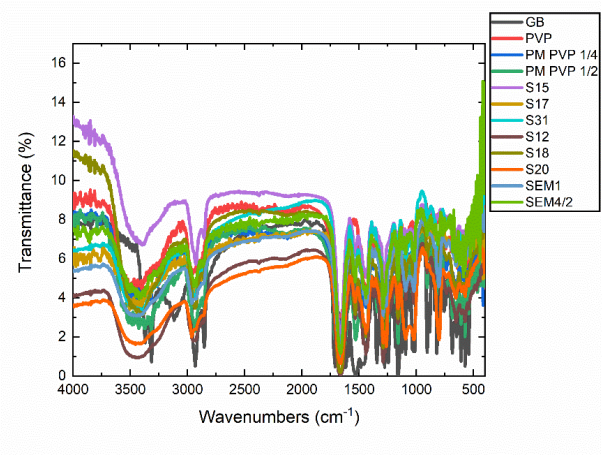

b

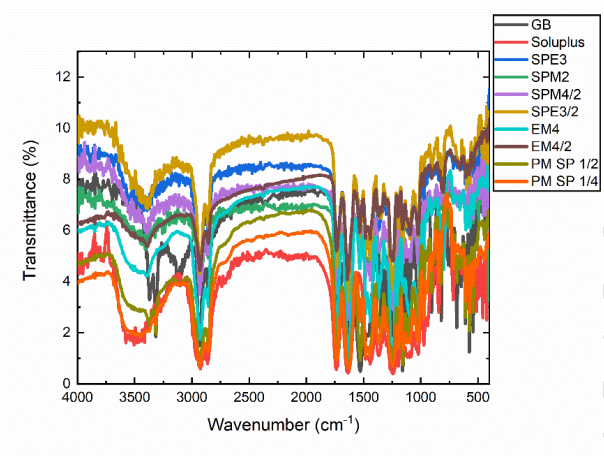

Fig. 4. FTIR spectra of (a) pure GB, PVP powder, physical mixture of GB/PVP (1:4) (w/w) PM PVP 1/4 & GB/PVP (1:2) (w/w) PM PVP 1/2, and (1:4) and (1:2) GB-PVP nanoparticles and (b) pure GB, SP powder, physical mixture of GB/SP (1:4) (w/w) PM SP 1/4 & GB/SP (1:2) (w/w) PM SP 1/2, and (1:4) and (1:2) GB-SP nanomicelles prepared with different solvents.

Chemometrics Studies:

Hierarchical cluster analysis (HCA): Clustering of samples in groups and sub-groups could be achieved through HCA. GB-PVP nanoparticles and GB-SP nanomicelles samples are shown in (Fig. 5 a & b), respectively. By using their spectra, the samples clustered into two groups revealing the intra-group similarity. The spectral range difference was assessed based on deeming groups of similar areas in all the samples. The HCA dendrograms gave a rough idea about the differences in the composition of the nanoparticles and the nanomicelles. To fully diagnose the variations in the functional group between the samples that cause the difference in the HCA and to assess the vibrations alter of different functional groups in terms of their intensity and shift, principal component analysis (PCA) was used [36].

a

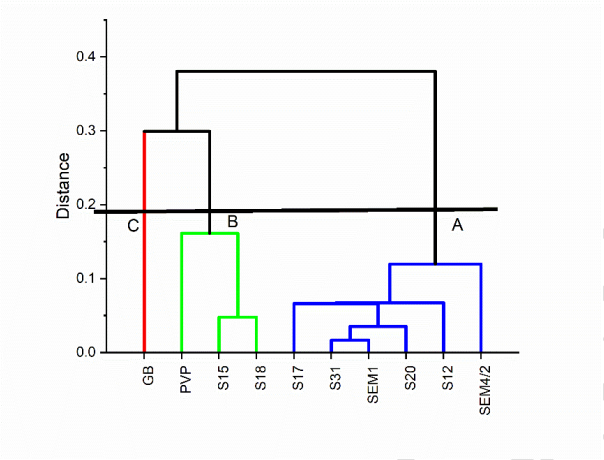

b

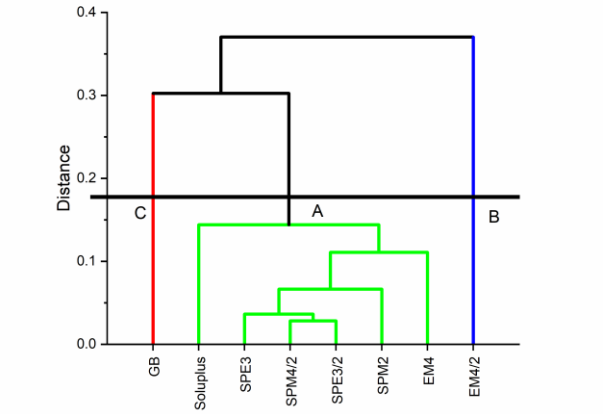

Fig. 5. Hierarchical Cluster Analysis (HCA) for FTIR Spectra of (a) GB-PVP nanoparticles and (b) GB-SP nanomicelles.

Principal Component Analysis (PCA): PCA is frequently employed to treat the spectral data comprising of thousands of variables that demand data reductions. The reduced variables are called principal components (PCs). PCs are orthogonal linear combinations of the original

variables that effectively state data variability in low dimensions [37]. The calculations given by PCs account for the highest percentage of the variance. As depicted in (Supplementary Fig. S1 and Fig. S2), the most impact on the variance of the analyzed FTIR spectrums was correlated with the first two PCs for both GB-PVP nanoparticles and GB-SP nanomicelles. PCA gives score plots, where two PCs (e.g., PC1 vs. PC2) are presented and where the analyzed samples are taking specific positions (scores) to form clusters of similar compounds [37]. The FTIR samples were grouped based on the outcomes of the PCA to visualize their position, from GB and the polymer, the score plot of GB-PVP nanoparticles and GB-SP nanomicelles are shown in (Fig. 6 a & b).

Nanoparticles were classified into two groups: Group A on the right side of the score plot was well separated from Group B, including S_{15} and S_{18} based on their position from PVP in PC1, explaining the 72.8% of the variance. It denotes the dominant of PVP in the nanoparticles, where the samples S_{18} and S_{15} showed positive score plots in PC2 signifying the more GB contribution in the formulations, explaining the 18.2 % of the variance. It is worth mentioning that samples S_{18} and S_{15} are of GB loading of 50%. Also, the samples were scattered within the score plot may be referred to the use of different solvents mixtures which contributed to structuring the electrosprayed nanoparticles.

The GB-SP nanomicelles were clustered into two groups (Fig. 6 b), Group A (circled in red) and Group B (circled in yellow), as they were closer to Soluplus than GB in PC1, which clarify the 83.7% of the variance. It indicates that Soluplus® is the most abundant constituent in the nanomicelles. While in PC2, samples of $SPE_{3/2}$ and $SPM_{4/2}$ with richer drug content were nearer to GB, clarifying the 9.2% of the variance. Forming its one-element cluster, sample $EM_{4/2}$ showed the highest intensity among the nanomicelles, which elucidated such an organization in

Formatted: Superscript

groups of samples [36]. The PCA demonstrated the adequate encapsulation of the drug within the polymer matrix.

a

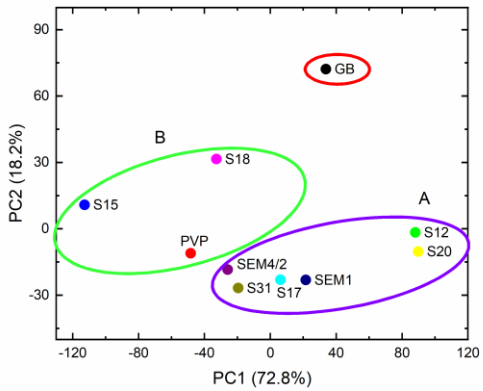

b

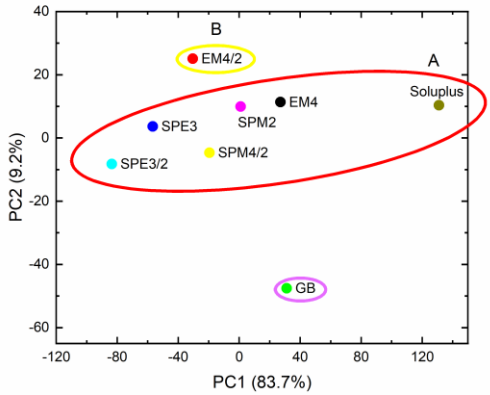

Fig. 6. Results of principal component analysis (PCA), displayed as a score plot~~, performed~~. performed on the matrix collecting spectral data of (a) GB, PVP, and 1:4 and 1:2 GB-PVP nanoparticles and (b) GB, SP, and 1:4 and 1:2 GB-SP nanomicelles.

3.4 Zeta Potential:

The zeta potential values of GB-PVP nanoparticles and GB-SP nanomicelles are displayed in (Table. 3). The zeta potentials of the GB-SP nanomicelles were neutral [38]. It was expected, in consequence, of a non-ionic hydrophilic polymer polyethylene glycol (PEG) in the micelles shell [16]. In agreement with other results on PEGylated nanosystems, after intravenous administration, a hydrophilic and neutral surface charge minimizes the formation of protein corona and augments the circulation time [39].

3.5 Cloud Point:

The temperature at which a homogenous amphiphilic polymer solution displays a cloudy appearance is called the cloud point [16]. The reason for this phenomenon is the dehydration of the hydrophilic part of the polymers due to the temperature increase, which causes the micelles to be unstable and aggregate [40], where the cloud point aids in selecting the storage conditions and estimating the stability of the formulation after administration [15]. The GB-SP nanomicelles of the different solvents mixtures exhibited a cloud point of 36.5 ± 0.6 ˚C, which is in consistent with the previous reports [40].

3.6 *In vitro* drug release studies:

Formatted: Font: Italic

The use of PVP and SP polymers brought up different drug release behavior of the electrosprayed particles. The solvents' effect on producing nanostructures of various physicochemical properties has an impact on the dissolution of the particles in the media of PH (7.4) PBS. Sink condition was maintained by keeping the ratio between the donor (dialysis bag) and the receptor (bulk media) at 1/20 (v/v) [41], [42]. This release media was designed to diverse

and signify the release of the different electrosprayed nanoparticles. The addition of a surfactant would affect the particles' dissolution rate as it will interfere with the nanoparticle's structure and stability [41]. The nanoparticles were always in a supersaturated concentration three times above the saturated solubility of GB of 0.018 mg ml^{-1}. The GB-PVP nanoparticles and the GB-SP nanomicelles showed high %EE and %DL (Table. 3), denoting that the drug loading in the particles is close to the amount added to the feed solution before electrospraying.

The GB-PVP nanoparticles fabricated using different solvents mixtures exhibited varied drug release (Fig. 7 a). Most of the particles were released within the early minutes, then a drop in dissolution rate took place to suggest the drug recrystallization, this is due to the hydrophilic nature of PVP where a drug supersaturation attained rapidly and declined shortly [43]. The nanoparticles S_{31}, S_{20}, and SEM_1 formulated with DCM solvent mixtures exhibited the highest and fastest dissolution rate. The solubility of GB and PVP in DCM is better than in Act, which distributes the drug more uniformly, although all the nanoparticles were amorphous, as the XRPD and FTIR tests showed. The sample S_{31} formulated with DCM/MeOH solvent mixture reached the complete release in 45 minutes, regarding their small size ~~of 429~~of 429 nm (Table. 3) and spherical morphology. While the lower GB loading sample ~~S_{20} formulated~~S_{20} formulated with the same mixture released 88.8 ± 1.48% in ten minutes and dropped away afterward due to the large, broad size distribution and agglomerated particles. The Act/Eth fabricated samples of S_{12} and S_{18} demonstrated burst release of 78.8 ± 2.62% and 92.9 ± 3.45~~% at~~% at 1 hour, for GB loading of 25% and 50% (w/w), respectively. The same trend was adapted as the 50% drug loading induced the higher drug release. The nanoparticles of Act/MeOH, samples S_{14} and S_{15}, displayed a lower dissolution rate suggesting the poor solvents mixture.

Nanomicelles of GB-SP exhibited a more controlled dissolution rate than GB-PVP

nanoparticles (Fig. 7 b). Consisting of both hydrophilic and lipophilic polymers tend to form micelles in the release media, stabilizing the drug in the supersaturated state and inducing a more sustained release. The nanomicelles exhibited a burst release for the first two hours followed by a sustained release, the lower SP content nanomicelles displayed sustained drug release till 12 hours, then the drug release dropped away (Supplementary Fig. S3), while the richer SP nanomicelles continued elevating to reach 96.5% ± 0.23, 94.2% ± 0.47, and 95.9% ± 0.38 for EM_4, SPE_3, and SPM_2, respectively. The amphiphilic polymers kept the drug in a supersaturated colloidal system, as the drug to polymer ratio plays a key role in supersaturation maintaining. Increasing the drug loading compromised both the drug release and the supersaturation maintenance [43].

The use of solvents mixtures participated in delivering nanoparticles and nanomicelles of different inherent properties and that is demonstrated in the drug release curves. Parenteral administration of these particles implies its higher bioavailability but also the controlled release and the intensity to site targeting are of equal importance. In this regard, GB-SP nanomicelles are of the upper hand. The drug release could be designed to be sustained and eliminate the repetition of the dose administration. That is the case of SPE_3, SPM_2, and EM_4 (Fig. 7 b), where GB released gradually to reach about 80% of the total dose at 24 hours. The linear and the gradual trend of the release denotes that these nanomicelles could release the drug for a prolonged time, while the impede of rapid release at the early hours could prohibit the degradation of GB during the delivery and blood circulation [15]. The high drug encapsulation and the strong drug affinity toward the hydrophobic core of the nanomicelles could explicate the drug behavior. GB-SP nanomicelles represent a promising vehicle for drug delivery keeping the

drug particles in a solid solution preventing the recrystallization or the precipitation of the drug molecules, which could be observed with GB-PVP particles.

The cumulative release data were fitted with different kinetic mathematical models to understand the GB release mechanism from the nanomicelles. The full release mechanism from the supramolecules could not be described by a model which concurrently takes into account the structure and properties of the excipient, besides the drug features and the interactions that may be created among each other. The drug release from the nanomicelles could be due to different release mechanisms, such as micelle relaxation, unimer dissociation, and molecular diffusion [37]. In this regard, a model which fitted the release data well is selected. A linear regression analysis was run for each mathematical model, and the one which showed the highest value denoting the coefficient of determination (R^2) was considered the best fit model of the drug release. The R^2 states the model strength to elucidate the data variability. The R^2 values are listed in (Table. 4). –Following these results, the zero order showed the best fit for the GB release of all the GB-SP nanomicelles, which means that the release is independent of the GB concentration and happens at a constant rate [44] .

Formatted: Indent: First line: 0.5"

a

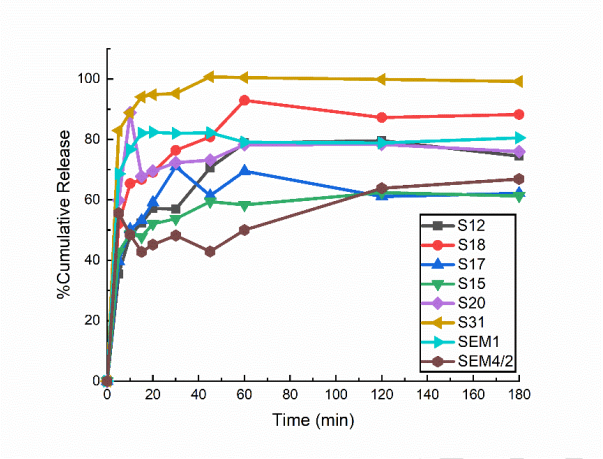

b

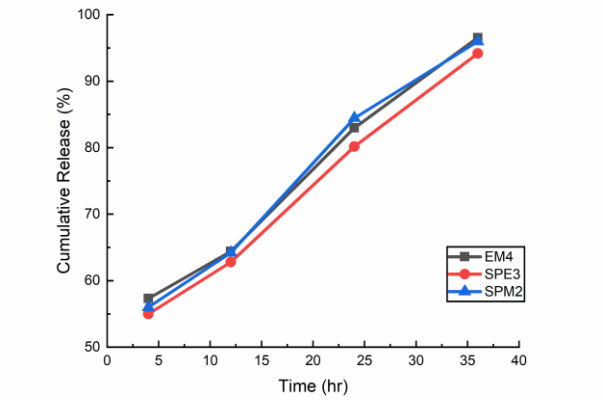

Fig. 7. Cumulative drug release % versus time from the (a) GB-PVP ~~1:4 and~~1:4 and 1:2 (w/w) and (b) GB-SP ~~1:4 (~~1:4 (w/w) formulations suspension in PBS.

Table 4. R^2 values obtained after fitting the drug release data to various release kinetic models.

Sample No.	Zero order		First order		Higuchi		Korsmeyer-Peppas		Baker-Lonsdale	
	R^2	Slope	R^2	Slope	R^2	Slope	R^2	Slope	R^2	Slope
SPE_3	0.996	0.492	0.937	0.349	0.969	0.322	0.928	0.241	0.991	0.899
SPM_1	0.995	0.498	0.916	0.268	0.964	0.325	0.919	0.242	0.988	0.898
EM_1	0.993	0.512	0.918	0.266	0.964	0.341	0.917	0.236	0.989	0.889

4. Conclusions:

The electrospraying process established its uniqueness in delivering different drug loading nanoparticles intended for varied medicinal use. Considering that stability is essential for any drug delivery system, the dry powder is used to increase the physical and chemical constancy of the formulations over a prolonged time and facilitate the storage conditions. Thus, the design of glibenclamide nanoparticles as dry powder reconstituted for parenteral use was implemented by electrospraying. Setting two polymers of different nature developed particles of various physicochemical properties, this was emphasized in the drug release. The solvents mixtures gave varied morphology of GB-PVP nanoparticles and GB-SP nanomicelles. While, the Act/Eth gave the smallest GB-PVP nanoparticles, a spherical morphology, and somewhat high drug release, whereas the DCM/MeOH solvents mixture showed the spherical, small size, and drug release for the 50% drug loading particles. The GB-SP nanomicelles were of different morphology, with a size range from (447-750~~) nm~~) nm, and are amorphous as the XRD and FTIR showed. The drug release of the nanomicelles was less influenced by the type of solvent used, as the amphiphilic polymer ratio was the criterion. Soluplus formed nanomicelles at 36.5 °C, which is the temperature of the physiological body fluids, capturing the hydrophobic glibenclamide in the

Formatted: Justified

core while the shell with the hydrophilic PEG polymer act as a protector and provides the environment for the drug diffusion. The glibenclamide/Soluplus ratio of 1:4 (w/w) was the proper ratio to assure sustained release for up to 36 hours. The electrosprayed nanoparticles were dispersed easily in distilled water to get a clear solution merely by mild shaking, enduring their ready-to-use. The solvent mixture governs the size of the nanoparticles concerning the electrical conductivity, demonstrating that GB-PVP nanoparticles were shaped in varied morphology depending on the type of the solvent, the drug/ polymer ratio, and the solubility of PVP. The Soluplus® amphiphilic polymer forming a core-shell structure with the drug encapsulated inside the hydrophobic core regulates the drug release, and the hydrophilic shell with neutral zeta potential extended the blood circulation time and the nanomicelles stability. The GB-SP nanomicelles represent a great candidate for the glibenclamide injection formula.

Formatted: Superscript

COMPETING INTERESTS DISCLAIMER:

Authors have declared that no competing interests exist. The products used for this research are commonly and predominantly use products in our area of research and country. There is absolutely no conflict of interest between the authors and producers of the products because we do not intend to use these products as an avenue for any litigation but for the advancement of knowledge. Also, the research was not funded by the producing company rather it was funded by personal efforts of the authors.

References:

[1] M. P. Desai, V. Labhasetwar, E. Walter, R. J. Levy, and G. L. Amidon, "The mechanism of uptake of biodegradable microparticles in Caco-2 cells is size dependent," *Pharmaceutical Research*, vol. 14, no. 11. pp. 1568–1573, 1997, doi: 10.1023/A:1012126301290.

[2] Y. Yang, D. Nie, Y. Liu, M. Yu, and Y. Gan, "Advances in particle shape engineering for improved drug delivery," *Drug Discov. Today*, vol. 24, no. 2, pp. 575–583, 2019, doi: 10.1016/j.drudis.2018.10.006.

[3] L. V. V. Nguyen and P. D. Huynh, "Controlling the morphology of polycaprolactone microparticles produced by electrospraying," *Sci. Technol. Dev. J. - Nat. Sci.*, vol. 1, no. T4, pp. 130–137, 2017, doi: 10.32508/stdjns.v1it4.477.

[4] S. Zhang, C. Campagne, and F. Salaün, "Influence of solvent selection in the electrospraying process of polycaprolactone," *Appl. Sci.*, vol. 9, no. 3, 2019, doi: 10.3390/app9030402.

[5] H. Lee, S. An, S. Kim, B. Jeon, M. Kim, and I. S. Kim, "Readily Functionalizable and Stabilizable Polymeric Particles with Controlled Size and Morphology by Electrospray," *Sci. Rep.*, vol. 8, no. 1, pp. 1–10, 2018, doi: 10.1038/s41598-018-34124-0.

[6] Z. Yang, H. Peng, W. Wang, and T. Liu, "Crystallization behavior of poly(ε-caprolactone)/layered double hydroxide nanocomposites," *J. Appl. Polym. Sci.*, vol. 116, no. 5, pp. 2658–2667, 2010, doi: 10.1002/app.

[7] Y. Q. Wu and R. L. Clark, "Controllable porous polymer particles generated by electrospraying," *J. Colloid Interface Sci.*, vol. 310, no. 2, pp. 529–535, 2007, doi: 10.1016/j.jcis.2007.02.023.

[8] R. P. A. Hartman, D. J. Brunner, D. M. A. Camelot, J. C. M. Marijnissen, and B. Scarlett, "Jet break-up in electrohydrodynamic atomization in the cone-jet mode," *J. Aerosol Sci.*, vol. 31, no. 1, pp. 65–95, 2000, doi: 10.1016/S0021-8502(99)00034-8.

[9] H. Wei and R. Löbenberg, "Biorelevant dissolution media as a predictive tool for

glyburide a class II drug," *Eur. J. Pharm. Sci.*, vol. 29, no. 1, pp. 45–52, 2006, doi: 10.1016/j.ejps.2006.05.004.

[10] R. M. Jha *et al.*, "Glibenclamide Treatment in Traumatic Brain Injury: Operation Brain Trauma Therapy," *J. Neurotrauma*, vol. 38, no. 5, pp. 628–645, 2021, doi: 10.1089/neu.2020.7421.

[11] J. M. Simard *et al.*, "Newly expressed SUR1-regulated NCCa-ATP channel mediates cerebral edema after ischemic stroke," *Nat. Med.*, vol. 12, no. 4, pp. 433–440, 2006, doi: 10.1038/nm1390.

[12] V. Gerzanich *et al.*, "Sulfonylurea receptor 1, transient receptor potential cation channel subfamily M member 4, and KIR6.2:Role in hemorrhagic progression of contusion," *J. Neurotrauma*, vol. 36, no. 7, pp. 1060–1079, Apr. 2019, doi: 10.1089/neu.2018.5986.

[13] D. W. Griepp, J. Lee, C. M. Moawad, C. Davati, J. Runnels, and B. Fiani, "BIIB093 (intravenous glibenclamide) for the prevention of severe cerebral edema," *Surg. Neurol. Int.*, vol. 12, no. 80, pp. 1–8, 2021, doi: 10.25259/SNI_933_2020.

[14] BASF, "Soluplus® Technical Information," *BASF, Pharma ingredients Serv.*, no. August, pp. 1–14, 2019.

[15] M. C. Bergonzi, M. Vasarri, G. Marroncini, E. Barletta, and D. Degl'Innocenti, "Thymoquinone-loaded soluplus®-solutol® HS15 mixed micelles: Preparation, in vitro characterization, and effect on the SH-SY5Y cell migration," *Molecules*, vol. 25, no. 20, pp. 1–17, 2020, doi: 10.3390/molecules25204707.

[16] V. Piazzini *et al.*, "Formulation of nanomicelles to improve the solubility and the oral absorption of silymarin," *Molecules*, vol. 24, no. 9, pp. 1–20, 2019, doi: 10.3390/molecules24091688.

[17] G. S. Kwon, "Polymeric Micelles for Delivery of Poorly Water-Soluble Compounds," *Crit. Rev. Ther. Drug Carr. Syst.*, vol. 20, no. 5, pp. 357–403, 2003, doi: 10.1615/CRITREVTHERDRUGCARRIERSYST.V20.I5.20.

[18] Z. K. Nagy *et al.*, "Comparison of electrospun and extruded soluplus®-based solid dosage forms of improved dissolution," *J. Pharm. Sci.*, vol. 101, no. 1, pp. 322–332, Jan. 2012, doi: 10.1002/JPS.22731.

[19] S. Y. Lee *et al.*, "Electrosprayed nanocomposites based on hyaluronic acid derivative and Soluplus for tumor-targeted drug delivery," *Colloids Surfaces B Biointerfaces*, vol. 145, pp. 267–274, 2016, doi: 10.1016/j.colsurfb.2016.05.009.

[20] U. Paaver *et al.*, "Soluplus graft copolymer: Potential novel carrier polymer in electrospinning of nanofibrous drug delivery systems for wound therapy," *Biomed Res. Int.*, vol. 2014, pp. 14–18, 2014, doi: 10.1155/2014/789765.

[21] D. Lucio, J. M. Irache, M. Font, and M. C. Martínez-Ohárriz, "Supramolecular structure of glibenclamide and β-cyclodextrins complexes," *Int. J. Pharm.*, vol. 530, no. 1–2, pp. 377–386, 2017, doi: 10.1016/j.ijpharm.2017.08.002.

[22] Y. Wang *et al.*, "The role of particle size of glyburide crystals in improving its oral

absorption," *Drug Deliv. Transl. Res.*, vol. 7, no. 3, pp. 428–438, 2017, doi: 10.1007/s13346-017-0378-3.

[23] S. Maritim, P. Boulas, and Y. Lin, "Comprehensive analysis of liposome formulation parameters and their influence on encapsulation, stability and drug release in glibenclamide liposomes," *Int. J. Pharm.*, vol. 592, 2021, doi: 10.1016/j.ijpharm.2020.120051.

[24] S. Chuangchote, T. Sagawa, and S. Yoshikawa, "Electrospinning of poly(vinyl pyrrolidone): Effects of solvents on electrospinnability for the fabrication of poly(p-phenylene vinylene) and TiO2 nanofibers," *J. Appl. Polym. Sci.*, vol. 114, no. 5, pp. 2777–2791, Dec. 2009, doi: 10.1002/APP.30637.

[25] I. Smallwood, *Handbook of organic solvent properties*. London :;New York : Arnold ;;Halsted Press, 1996.

[26] J. Luecke and R. L. Mccormick, "Electrical Conductivity and pH," *Energy & Fuels*, vol. 28, pp. 5222–5228, 2014.

[27] M. Cagel *et al.*, "Mixed micelles for encapsulation of doxorubicin with enhanced in vitro cytotoxicity on breast and ovarian cancer cell lines versus Doxil®," *Biomed. Pharmacother.*, vol. 95, no. August, pp. 894–903, 2017, doi: 10.1016/j.biopha.2017.09.006.

[28] K. H. Lee, H. Y. Kim, M. S. Khil, Y. M. Ra, and D. R. Lee, "Characterization of nano-structured poly(1-caprolactone) nonwoven mats via Electrospinning," *Polymer (Guildf).*, vol. 44, pp. 1287–1294, 2003.

[29] A. Bohr *et al.*, "Pharmaceutical microparticle engineering with electrospraying: the role of mixed solvent systems in particle formation and characteristics," *J. Mater. Sci. Mater. Med.*, vol. 26, no. 2, pp. 1–13, 2015, doi: 10.1007/s10856-015-5379-5.

[30] A. M. Gañán-Calvo, "Cone-jet analytical extension of Taylor's electrostatic solution and the asymptotic universal scaling laws in electrospraying," *Phys. Rev. Lett.*, vol. 79, no. 2, pp. 217–220, 1997, doi: 10.1103/PhysRevLett.79.217.

[31] J. Yao, L. Kuang Lim, J. Xie, J. Hua, and C. H. Wang, "Characterization of electrospraying process for polymeric particle fabrication," *J. Aerosol Sci.*, vol. 39, no. 11, pp. 987–1002, 2008, doi: 10.1016/j.jaerosci.2008.07.003.

[32] P. G. Takla, "Glibenclamide," *Anal. Profiles Drug Subst. Excipients*, vol. 10, no. C, pp. 337–355, Jan. 1981, doi: 10.1016/S0099-5428(08)60644-9.

[33] P. Liu *et al.*, "Soluplus-mediated diosgenin amorphous solid dispersion with high solubility and high stability: Development, characterization and oral bioavailability," *Drug Des. Devel. Ther.*, vol. 14, pp. 2959–2975, 2020, doi: 10.2147/DDDT.S253405.

[34] A. Homayouni, F. Sadeghi, A. Nokhodchi, J. Varshosaz, and H. A. Garekani, "Preparation and characterization of celecoxib dispersions in soluplus®: Comparison of spray drying and conventional methods," *Iran. J. Pharm. Res.*, vol. 14, no. 1, pp. 35–50, 2015, doi: 10.22037/ijpr.2015.1621.

[35] R. N. Shamma and M. Basha, "Soluplus®: A novel polymeric solubilizer for optimization of Carvedilol solid dispersions: Formulation design and effect of method of preparation," *Powder Technol.*, vol. 237, pp. 406–414, 2013, doi: 10.1016/j.powtec.2012.12.038.

[36] A. Matwijczuk *et al.*, "Use of FTIR spectroscopy and chemometrics with respect to storage conditions of Moldavian Dragonhead Oil," *Sustain.*, vol. 11, no. 22, 2019, doi: 10.3390/su11226414.

[37] G. Zuccari *et al.*, "Increased water-solubility and maintained antioxidant power of resveratrol by its encapsulation in vitamin E TPGS micelles: A potential nutritional supplement for chronic liver disease," *Pharmaceutics*, vol. 13, no. 8, 2021, doi: 10.3390/pharmaceutics13081128.

[38] J. D. Clogston and A. K. Patri, "Zeta potential measurement.," *Methods Mol. Biol.*, vol. 697, pp. 63–70, 2011, doi: 10.1007/978-1-60327-198-1_6.

[39] M. Ghezzi *et al.*, "Polymeric micelles in drug delivery: An insight of the techniques for their characterization and assessment in biorelevant conditions," *J. Control. Release*, vol. 332, no. January, pp. 312–336, 2021, doi: 10.1016/j.jconrel.2021.02.031.

[40] E. Bernabeu, L. Gonzalez, M. Cagel, E. P. Gergic, M. A. Moretton, and D. A. Chiappetta, "Novel Soluplus®-TPGS mixed micelles for encapsulation of paclitaxel with enhanced in vitro cytotoxicity on breast and ovarian cancer cell lines," *Colloids Surfaces B Biointerfaces*, vol. 140, pp. 403–411, 2016, doi: 10.1016/j.colsurfb.2016.01.003.

[41] S. Hua, "Comparison of in vitro dialysis release methods of loperamide-encapsulated liposomal gel for topical drug delivery," *Int. J. Nanomedicine*, vol. 9, no. 1, pp. 735–744, 2014, doi: 10.2147/IJN.S55805.

[42] S. D'Souza, " A Review of In Vitro Drug Release Test Methods for Nano-Sized Dosage Forms ," *Adv. Pharm.*, vol. 2014, pp. 1–12, 2014, doi: 10.1155/2014/304757.

[43] R. Peng *et al.*, "Polymer/lipid interplay in altering in vitro supersaturation and plasma concentration of a model poorly soluble drug," *Eur. J. Pharm. Sci.*, vol. 146, no. January, 2020, doi: 10.1016/j.ejps.2020.105262.

[44] "Mathematical models of drug release," *Strateg. to Modify Drug Release from Pharm. Syst.*, pp. 63–86, 2015, doi: 10.1016/b978-0-08-100092-2.00005-9.

List of Figures:

Fig. 5. Hierarchical Cluster Analysis (HCA) for FTIR Spectra of (a) GB-PVP nanoparticles and (b) GB-SP nanomicelles.

Fig. 6. Results of principal component analysis (PCA), displayed as a score plot, performed on the matrix collecting spectral data of (a) GB, PVP, and 1:4 and 1:2 GB-PVP nanoparticles and (b) GB, SP, and 1:4 and 1:2 GB-SP nanomicelles.

Fig. 7. Cumulative drug release % versus time from the (a) GB-PVP 1:4 and 1:2 (w/w) and (b) GB-SP 1:4 (w/w) formulations suspension in PBS.

Supplementary Fig. S1. Plot of eigenvalues, scree plot, for PCA of FTIR spectra of GB, PVP, and 1:4 and 1:2 GB-PVP nanoparticles.

Supplementary Fig. S2. Plot of eigenvalues, scree plot, for PCA of FTIR spectra of GB, SP, and 1:4 and 1:2 GB-SP nanomicelles.

Supplementary Fig. S3. Cumulative drug release % versus time from the GB-SP 1:4 and 1:2 (w/w) formulations.

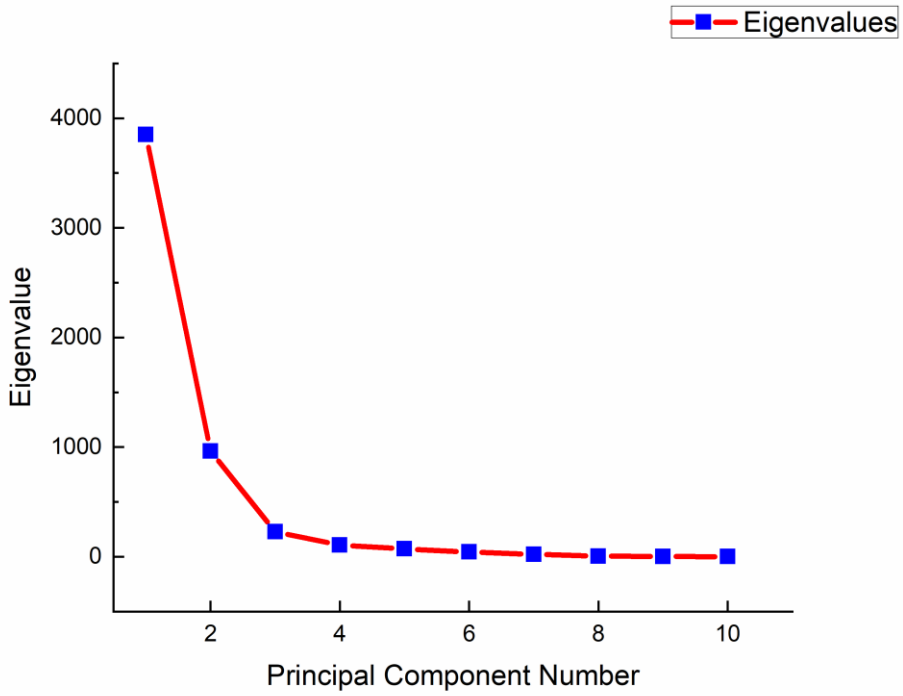

Supplementary Fig. S1. Plot of eigenvalues, scree plot, for PCA of FTIR spectra of GB, PVP, and 1:4 and 1:2 GB-PVP nanoparticles.

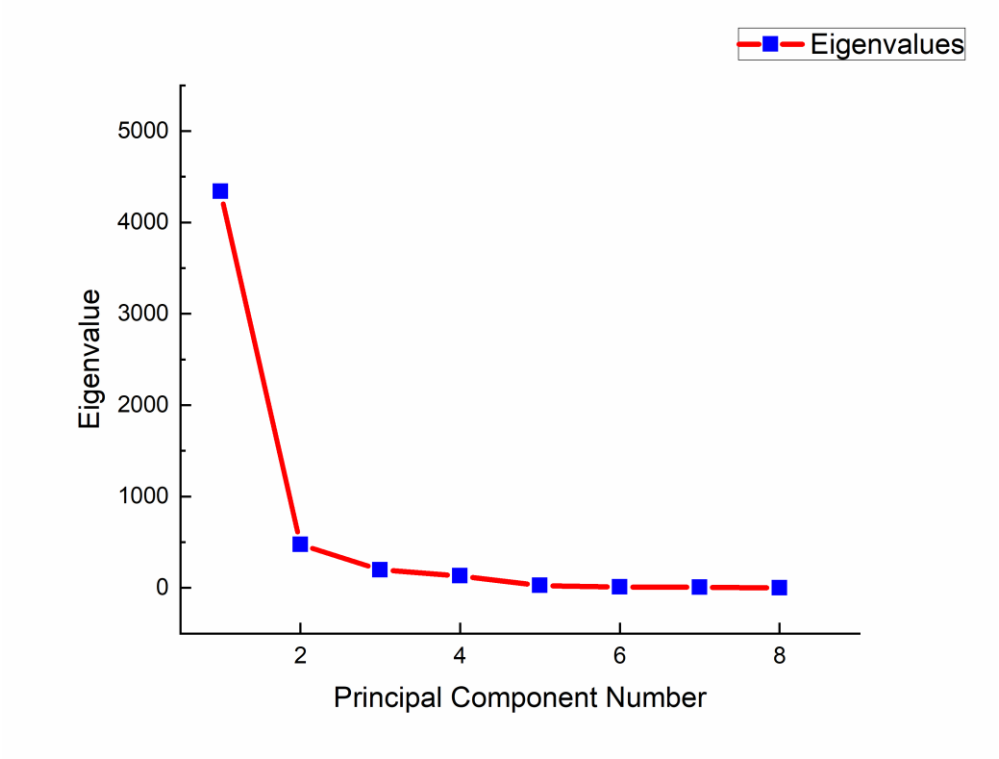

Supplementary Fig. S2. Plot of eigenvalues, scree plot, for PCA of FTIR spectra of GB, SP, and 1:4 and 1:2 GB-SP nanomicelles.

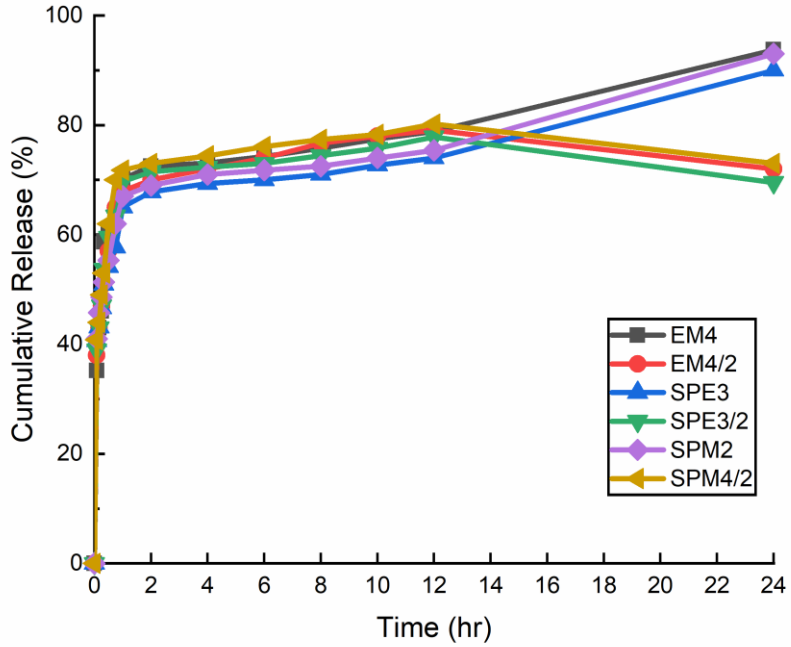

Supplementary Fig. S3. Cumulative drug release % versus time from the GB-SP 1:4 and ~~1:2 (~~1:2 (w/w) formulations.

Declaration of interests

☒ The authors declare that they have no known competing financial interests or personal relationships that could have appeared to influence the work reported in this paper.

☐The authors declare the following financial interests/personal relationships which may be considered as potential competing interests: